Peptide targeting and imaging of damaged lung tissue in influenza-infected mice

Peptide Targeting and Imaging of

Damaged Lung Tissue in Influenza-Infected Mice

Authors: Na Li[1, 2], Lu Yin[1], Damien Thévenin[3], Yoshiyuki Yamada[1], Gino Limmon[1], Jianzhu Chen[4], Vincent TK Chow[2], Donald M. Engelman[3], Bevin P. Engelward[5*]

1 Interdisciplinary Research Group in Infectious Diseases, Singapore-Massachusetts Institute of Technology Alliance in Research and Technology

Address: 1 CREATE Way, #03-12/13/14 Enterprise Wing, Singapore 138602

2 Department of Microbiology, National University of Singapore

Address: 5 Science Drive 2, Block MD4 Level 3, Singapore 117597

3 Department of Molecular Biophysics & Biochemistry, Yale University

Address: 266 Whitney Avenue, P.O. Box 208114, New Haven, CT 06520-8114

4 The David H. Koch Institute for Integrative Cancer Research at MIT

Address: 500 Main Street, MIT building 76-243, Cambridge, MA 02142

5 Department of Biological Engineering, Massachusetts Institute of Technology

Address: Building 56, Room 631, 77 Massachusetts Ave., Cambridge (MA) 02139

Corresponding author: Bevin P. Engelward

*email: bevin@mit.edu

Competing interests: The authors have declared that no competing interests exist.

Author contributions

Conceived and designed the experiments: NL, BPE. Performed the experiments: NL Analysed the data: NL, LY. Design of quantification algorithms: LY. Peptide-fluorophore conjugate synthesis: DT. Contributed materials/analysis tools: YY, GVL, VTKC, DE, JC BPE. Wrote the paper: NL, BPE.

Summary (144)

Aim. In this study, we investigate whether the pH (Low) Insertion Peptide (pHLIP®) can target regions of lung injury associated with influenza infection. **Materials and methods.** Fluorophore-conjugated pHLIP is injected i.p. into mice infected with a sublethal dose of H1N1 Influenza and visualized histologically. **Results.** pHLIP specifically targets inflamed lung tissues of infected mice in the later stages of disease and at sites where alveolar type I and type II cells are depleted. Regions of pHLIP-targeted lung tissue are devoid of peroxiredoxin 6, the lung-abundant antioxidant enzyme, and are deficient in pneumocytes. Interestingly, a pHLIP variant possessing mutations that renders it insensitive to pH changes was also able to target damaged lung tissue. **Conclusion.** pHLIP holds a potential for delivering therapeutics for lung injury during influenza infection. Furthermore, there may be more than one mechanism that enables pHLIP variants to target inflamed lung tissue.

Keywords: Influenza, inflammation, pHLIP, peptide, delivery

Introduction

Many influenza-related deaths are not directly linked to virus infection, but instead can be attributed to an exaggerated or dysregulated immune response towards the pathogenic insult [1] [2]. Hence, effective delivery of therapeutic agents aimed at ameliorating lung injury that is exacerbated by inflammation could greatly improve the survival and recovery of patients severely infected with influenza.

In this study, we set out to develop a strategy for targeting inflamed or injured regions of the lungs in order to enable delivery of pharmaceutical agents. It was previously reported that a ~36 amino acid pH-responsive peptide is able to target inflamed arthritic joints in mice [3]. This peptide, named 'pH (Low) Insertion Peptide', or in short, pHLIP® (pHLIP), has a strong affinity for low pH microenvironments such as tumors [4-6], where it inserts into cell membrane with a change in conformation and release of approximately 2 kcal/mole of energy. The energy released supports translocation of cargos conjugated to its C-terminus into the cytoplasm, making pHLIP a nanosyringe for small, cell-impermeable molecules such as phalloidin and peptide nucleic acid (PNA) [7-9]. While most healthy organs are usually slightly alkaline (~pH 7.2-7.4) under physiological conditions, the interstitium of inflamed tissue has a much lower pH (as low as pH 5.8) [10, 11]. Thus, influenza-induced lung inflammation may facilitate specific targeting of pHLIP. While extensive studies have been performed to evaluate pHLIP and to test its efficacy in the context of cancer, nothing had been done to test its utility as a means for targeted inflamed tissue associated with infection. Here, we have evaluated the ability of pHLIP to specifically target inflamed regions of the lung following infection with influenza.

To study pHLIP targeting of inflammation and associated lung injury, we examined the biodistribution of pHLIP in a C57Bl/6 murine model inoculated with an H1N1 variant of influenza, Influenza A/Puerto Rico/8/34 (PR8). High sublethal dose of PR8 infection in C57Bl/6 mice causes severe viral pneumonia, which is a principal characteristic of hospitalized or intensive care pandemic H1N1 patients [12-14]. Knowledge regarding the specific biodistribution of pHLIP is critical for evaluating its potential utility both as a bioimaging tool and as a delivery agent for therapeutic drugs. This study shows that pHLIP specifically targets inflamed lung tissue, and does not accumulate in non-inflamed lung tissue. pHLIP-targeted regions are devoid of healthy pneumocytes, indicating that pHLIP specifically targets damaged regions of the lung. Importantly, these regions are also deficient in Peroxiredoxin 6, an important lung-abundant antioxidant produced by ATI cells in response to inflammation. These findings bring about new possibilities for detecting inflammation-induced lung damage and for specific delivery of therapeutic agents, such as antioxidants, to regions of lung injury.

Interestingly, a peptide, known as K-pHLIP, similar to pHLIP but without the ability to behave in a pH responsive fashion was also able to target damaged lung tissue, suggesting the possibility of more than one mechanism by which pHLIP targeted damaged lung tissue during influenza. Together, these results suggest there is more than one mechanism for targeted delivery of pHLIP-conjugated agents to sites of pulmonary inflammation and lung injury.

Materials and Methods

- **Peptide synthesis and conjugation with fluorescent dye.**

The pHLIP peptide variant used in this study was synthesized with a cysteine residue at its N-terminus by solid-phase peptide synthesis and purified by reverse-phase HPLC at the W.M. Keck Foundation Biotechnology Resource Laboratory (Yale University). It has the following sequence: ACEQNPIYWARYADWLFTTPLLLLDLALLVDADEGTG. Fluorescent dyes were conjugated to the N-terminal cysteine of pHLIP using the following protocol: To a solution of pHLIP peptide (1 µmol) in a solvent mixture consisting of 1:1:3:5 of DMF, DMSO, methanol, and aqueous NH_4HCO_3 buffer (200 mM; pH 8) was added 1 eq. of Alexa Fluor® 647 C2 maleimide (Invitrogen) in 50 µL DMSO. This mixture was stirred at room temperature and in the dark for 10 minutes. To this reduced mixture, an oxidizing solution of $K_3Fe(III)CN_6$ (6 mg, 18.2 µmol, 23.1 eq.) in 60 µl of aqueous NH_4HCO_3 buffer (200 mM; pH 8) was added. This reaction mixture was stirred at room temperature for 3 hours. The desired product was isolated via reverse-phase HPLC (Hewlett Packard Zorbax semi-prep 9.4 x 250 mm SB-C18 column; flow rate: 2 mL/min; phase A: water + 0.01% TFA; phase B: acetonitrile + 0.01% TFA; gradient: 70 min from 99:1 A/B to 1:99 A/B). In subsequent experiments, Hylite Fluor 647-conjugated pHLIP and K-pHLIP (ACEQNPIYWARYAKWLFTTPLLLL**K**LALLVDADEGTG) was purchased from Anaspec. The purity was ≥90% as confirmed by analytical HPLC.

- **Animal Studies.**

This study was carried out in strict accordance with the National Advisory Committee for laboratory Animal Research (NACLAR) Guidelines (Guidelines on the Care and Use of Animals for Scientific Purposes) in facilities licensed by the Agri-Food and Veterinary Authority of Singapore (AVA), the regulatory body of the Singapore Animals and Birds Act. The protocol was approved by the Institutional Animal Care and Use Committee (IACUC), National University of Singapore (Permit Number: IACUC 117/10).

- **Viral infection.**

Eight- to twelve-week old female inbred C57Bl/6 mice were purchased from Biological Resource Centre (BRC) and CARE-NUS. All mice were housed in the animal vivarium at National University of Singapore (NUS). H1N1 Influenza A/Puerto Rico/8/34 (PR8) was propagated in chick embryos and titered with plaque assay. Mice were anaesthetized with 75 mg/kg of ketamine and 1 mg/kg of medatomidine were instilled intra-tracheally with 30 plaque-forming units (PFU)/75 µl/ mouse of PR8. They are then revived with 1mg/kg of antipamezole. Mice were monitored for 12 days for weight loss and disease symptoms.

- **Plaque assay of lung homogenates.**

Three uninfected or PR8-infected mice were sacrificed on day 5, day 7 and day 9 post infection. The cardiac lobes of mice lungs were frozen and homogenized in 400µl of PBS with gentle Macs and centrifuged at 10,000 rpm for 10 min at 4˚C. Cell free lung homogenate was used in the plaque assay. The PFU values were normalized against total protein (according to the Bradford assay).

- **Peptide administration and tissue collection.**

Mice were injected intra-peritoneally (IP) with 100µM (in 100µl) of fluorescently-labeled pHLIP or K-pHLIP on day 1, day 5 and day 10 post-infection. Two days after peptide injection, the mice were euthanized. Lungs, heart, spleen, liver and kidneys were harvested and fixed in 10% neutral-buffered formalin overnight at 4˚C. Fixed tissues were then dehydrated in sequentially higher concentration of ethanol and embedded in paraffin.

- **Histology and immunofluorescence.**

Transverse sections (5 µm) were de-waxed and rehydrated. Antigen retrieval was performed using proteinase K (20 ug/ml in TE Buffer, pH 8.0) and hot citric acid buffer treatment (10 mM Citric Acid, pH 6.0), as needed, depending upon the antibodies. Primary antibodies including anti-fibronectin (Sigma Aldrich), anti-Pdpn (R&D systems), anti-CCSP (Santa Cruz), anti-Prdx6 (Abcam) and anti-SPC (Santa Cruz). Antibodies were incubated overnight at 4˚C. Tissue sections were stained with Alexa Fluor 488- or Alexa Fluor 546-conjugated secondary antibodies (Molecular probes, Invitrogen) for 1 h at room temperature, washed and mounted with ProLong Gold Antifade with DAPI (Invitrogen). Fluorescence images were taken with Carl Zeiss scanning microscope, before counter-staining the tissue samples with H&E.

For wheat germ agglutinin (WGA) staining, tissue sections were dewaxed and rehydrated according to usual procedure. After 10 min, at 100^{o}C in hot citric acid buffer sections are stained for 1 h at room temperature with WGA-Alexa Fluor 488 (20 µg/ml, Molecular Probes, gift from Dr. T. Tan, Singapore-MIT Alliance for Research and Technology).

- **In vitro assay.**

Chamber slides were prepared with A549 cells (~$5x10^4$), cultured for 24 h, and rinsed twice with PBS adjusted to pH 5, 6, 7.4 and 8. Following incubation with 8 µM of 5-FAM-conjugated pHLIP in PBS with appropriate pH (30 min, room temperature, in the dark), cells were washed with the appropriate pH-adjusted PBS and viewed under a fluorescence microscope~~Following incubation with 8 µM of 5-FAM conjugated pHLIP in PBS with appropriate pH (30 min, room temperature, in the dark). cells were washed with the appropriate pH-adjusted PBS and viewed under a fluorescence microscope~~.

- **Feature extraction and pHLIP quantification.**

Infiltrated regions were identified by setting a threshold to segment darker stained regions of infiltrated regions from uninfiltrated regions based on images of H&E stained whole lung sections (N=3, 2 sections per mouse). Within the infiltrated region, a smaller threshold was then applied to demarcate heavily and moderately infiltrated regions. Masks of heavily infiltrated, moderately infiltrated, and uninfiltrated regions were generated. Details of the quantification algorithm are described in “Imaging-based Quantification of infiltration.”

Moderately infiltrated regions were confirmed at 20-40x magnification by thickening of alveolar walls, and presence of infiltration in the alveolar spaces that involves less than 70% of the total lung parenchyma. These regions were visibly distinguishable from heavily infiltrated sites, which are defined as densely stained regions with infiltration occupying more than 70% of the lung parenchyma.

Extent of colocalization of Alexa fluor 647-conjugated pHLIP with uninfiltrated, moderately and heavily infiltrated regions was assessed. Total pHLIP was identified by thresholding the intensity of each pixel in Alexa fluor 647-conjugated pHLIP containing images. Percentage of pHLIP in heavily infiltrated region, moderately infiltrated region and uninfiltrated regions are calculated by the ratio of pHLIP within each mask to total pHLIP respectively.

ATI cells were identified by thresholding the intensity of each pixel in tissue sections stained with anti-Pdpn. Holes among ATI cells, representing the alveolar spaces, were filled to form the mask of healthy areas; damaged areas were segmented by subtracting healthy areas from total lung sections. The percentage of pHLIP-positive pixels within healthy and damaged regions was computed. Two whole lung sections from each mouse (N=3 for uninfected and PR8-infected groups) were used for calculation. Similarly, Prdx6 positive regions were identified by thresholding Prdx6 intensity. The percentage of total pHLIP-induced pixels was calculated in Prdx6 positive regions and Prdx6 negative regions. All image processing and computation algorithms were performed with Matlab (The Math Works, Inc., Natick Massachusetts). The codes for the algorithms are available on request.

- **Imaging-based quantification of infiltration.**

Ten 5 µm thick transverse lung sections 50 µm apart each other were obtained from infected mice given or not given Hylite-Fluor 647 pHLIP. The sections were then stained with H&E and quantified for the percentage of lung tissue with severe infiltration or consolidation. Original RGB image of H&E stained tissue section was converted to

grayscale. One intensity threshold was set to exclude large empty spaces, including bronchi, trachea and large blood vessels, from total section area to obtain alveolar region. Another intensity threshold was set to segment regions of infiltrated lung parenchyma that are darkly stained with H&E from uninfiltrated regions that possess lightly stained lung parenchyma. The percentage was computed from regions of infiltration and total alveolar region. The Matlab algorithm used for this purpose is now reported in a manuscript under review.

- **Statistical Analysis.**

Each result is expressed as mean ± SEM (Standard error of mean) unless otherwise stated. Statistical analyses were performed by ANOVA or Student's *t* test. A value of $p < 0.05$ is considered to be statistically significant.

Results

- ***Infection and inflammation kinetics in PR8-infected mice***

Using an established influenza mouse model, here we explore the potential utility of pHLIP as a tool for controlling spatio-temporal delivery of therapeutic or imaging agents. C57Bl/6 mice were infected with a sublethal dose of H1N1 PR8. The infection kinetics of this model have been previously reported by our group and Kumar *et al.* These studies show that PR8-infected C57Bl/6 experience weight loss from day 4 post infection, and continue to lose weight until they reached minimum weights around day 10 to 11 post infection. This was also the time when maximal lung damage was observed. Thereafter, all mice survived and gradually regain pre-infection lung histology at day 21 post infection [15, 16].

In this model, viral titer rises quickly during the first few days, peaking at day five post infection (6.2 $x10^4$ PFU/mg of protein), thereafter the virus is rapidly reduced on day seven post infection (1.3 $x10^4$ PFU/mg of protein), with very little evidence of viral particles by day nine post infection (Fig 1A). Importantly, inflammation persists even after viral clearance. Inflammation in the lung tissue is observed histologically via presence of cellular infiltration that can readily be identified by high nuclear density of immune cells. There is a gradual increase in the amount of cellular infiltration into the lung parenchyma, which leads to condensed alveolar spaces towards the later stage of influenza infection. Consolidation of the alveoli is observed around day 11 post infection in which the alveolar spaces are densely packed with fluid and immune cells, as can be observed in H&E sections (Fig 1B). Since infection and inflammation are causes of

tissue acidification, we hypothesized that pHLIP could potentially target inflamed lung tissue.

- ***pHLIP targets influenza-infected lungs***

To test for pHLIP targeting to lung tissue affected by influenza-induced pneumonia, we conjugated Alexa Fluor 647 and Hylite Fluor 647 to pHLIP on its non-inserting N terminus to enable visualization of pHLIP in fresh or fixed tissue. Labeled pHLIP was administered on day 10 post infection and organs were harvested two days later to allow time for pHLIP to target the inflamed tissue and to clear from other tissues. No significant autofluorescence was observed in mice that did not receive pHLIP (Fig 2a and 2c), and there was no significant accumulation of pHLIP in the lungs of healthy mice (Fig 2b). On the other hand, we observed significant pHLIP-associated fluorescence in the lungs of infected mice (Fig 2d). Unconjugated Alexa Fluor 647 dye was also administered to mice (N=2) in the same molarity and no significant fluorescence can be detected in tissue sections of mice (data not shown).

- ***pHLIP colocalizes with region of infiltration***

Analysis of H&E stained lung tissue reveals that the severity of inflammation is highly variable throughout the lungs [intensity of nuclear staining (dark blue/purple) indicates the density of immune cell infiltration], wherein the most densely infiltrated regions are considered to be consolidated (Fig 2g and 2h). Hence, we proceeded to determine the extent to which the degree of cellular infiltration impacts pHLIP targeting. A comparison of the H&E stained tissue and the localization of pHLIP (compare Fig 2d

and 2h) shows that pHLIP co-localizes specifically to the densely infiltrated regions of the lung.

To quantify the association of pHLIP within regions of low and high infiltration, the degree of alveolar infiltration, and the percentage of pHLIP-induced fluorescence in total lung area were assessed. Using an in-house automated quantification program, we demarcated regions based upon the extent of infiltration by thresholding H&E images of whole-lung sections. The method is demonstrated in Figure 3A. Figure 3A has 4 columns in which the left most column is an image of the original H&E stained lung section. The quantification program first identifies heavily and moderately infiltrated regions which are traced out by blue lines shown in the second column. In each region, alveoli, bronchi and blood vessels are filled to generate an alveolar area (third column). Total pHLIP-induced fluorescence that overlaps with heavily and moderately infiltrated regions (right most column) was then quantified.~~Using an in-house automated quantification program, we demarcated regions based upon the extent of infiltration by thresholding H&E images of whole lung sections (Fig 3A). Heavily infiltrated and moderately infiltrated regions were traced (blue lines in right panels; top and bottom left images respectively) and the alveolar, bronchiolar or blood vessels were filled to generate masks over these regions (center images).~~ The total pHLIP-induced fluorescence found in these regions was quantified (right images). We calculated that only about 1% of pHLIP was in uninfiltrated regions, around 13% of pHLIP was in moderately infiltrated regions and around 85% of pHLIP was in heavily infiltrated regions (Fig 3B). This further confirms that pHLIP preferentially targets regions of infiltration. To find out whether pHLIP administration elevates infiltration, we quantified

the amount of infiltration in the lungs of infected mice as compared to infected mice injected with pHLIP. Results show that pHLIP does not increase amount of lung infiltration in infected mice lungs (Fig 3C). The data are consistent with our hypothesis that pHLIP targets inflamed tissues, which are likely to be acidified [4, 5].

Given the transient nature of severe inflammation, it seemed likely that the timing of pHLIP delivery would impact the extent of pHLIP targeting. We therefore asked whether pHLIP targets lung tissue at earlier times post infection by injecting pHLIP at 1 day and 5 days post infection (Fig S1A). Results show that pHLIP did not target the lungs of infected mice when administered one day post infection, and could be found in only one out of three mice if given five days post infection (Fig S1B). Our group previously reported PR8 infection of bronchiolar and alveolar epithelial cells during the early stages of infection and disappearance of influenza antigens by day 9 post infection [15]. Interestingly, immune cell infiltration was reduced in the lung parenchyma when viral infection was apparent. The lack of pHLIP in tissue during the window of virus replication suggests the infection alone does not facilitate entry of pHLIP into the lung tissue. Cellular inflammation may therefore be important in generating a microenvironment that enables pHLIP targeting of damaged lung tissue.

- ***Subcellular location of pHLIP***

Previous studies have shown that pHLIP inserts into membranes in a pH dependent fashion [17, 18]. Here, we tested the ability of pHLIP to specifically bind to human lung adenocarcinoma cells. As shown in Fig 4A, pHLIP indeed binds to the surface of the A549 cells in a pH dependent fashion. Consistent with these observations, pHLIP also bound to Raji cells (a B lymphoma cell line) at low pH (data

not shown). To explore the possibility that pHLIP is extracellular *in vivo*, we visualized fibronectin, a protein present in inflamed lung tissue within the extracellular matrix (ECM). Interestingly, some pHLIP can also be found in the same regions of polymerized fibronectin (Fig 4B). This result shows that pHLIP is indeed extracellular, and suggests that pHLIP may be on the surface of cells and also within the ECM, possibly as a result of entrapment.

To more specifically visualize cell membranes, we stained infected lungs for membrane glycoproteins using wheat germ agglutinin (WGA), which is pseudocolored green in Fig 4C. In the heavily infiltrated regions, some pHLIP is found sandwiched in between WGA, colocalized with WGA or at the boundaries of DAPI stains, suggesting close proximity to the cell membranes. Although it is difficult to discern specific binding of pHLIP at cell membranes, fluorophores conjugated to pHLIP that are singly inserted into cell membranes are not likely to be easily detected by epifluorescent or confocal microscopy. Given that pHLIP inserts into cell membranes at low pH, it is likely that pHLIP is also inserted into cell membranes at the sites of infiltration.

- ***pHLIP colocalizes with damaged lung tissue***

The alveolar spaces within the lungs are populated with pneumocytes that are required for gaseous exchange. We investigated the association of pHLIP with two pneumocytes: alveolar type I (ATI) and alveolar type II (ATII). Each cell type can be visualized via secondary staining of antibodies for cell type-specific markers: podaplanin (Pdpn) for ATI cells and C-terminus of surfactant protein C (SPC) for ATII cells. Fig 5A shows that, in influenza-infected lungs, ATI and ATII are prominently present throughout the alveolar parenchyma (stained yellow and green, respectively) in healthy portions of

the lung. In contrast, pHLIP is clearly concentrated in regions of severe infiltration that are largely devoid of Pdpn-positive ATI and SPC-positive ATII cells (darker regions).

Narasaraju *et al.* described that the loss of continuity in Pdpn (also known as T1-α) immunostaining in mouse lung parenchyma is an indication of type I pneumocyte damage [19]. Using a program that we designed to enable quantification of staining intensity and extent of overlay (see methods), the percent of pHLIP-derived pixels in Pdpn-positive and Pdpn-negative areas were quantified. While 84% of pHLIP coincides with Pdpn-negative areas, only 16% of pHLIP is found in Pdpn-positive areas (Fig 5B). Fig 5C demonstrates the method of quantification. It shows that uninfected lung (top panel) is entirely stained Pdpn positive (Pdpn+ area, column 3) and pHLIP is not detected in the uninfected lung (Total pHLIP, columns 2). In infected mouse lungs (bottom panel), pHLIP (Total pHLIP, column 2) does not greatly overlap with the Pdpn positive regions (Pdpn+ area, column 3); the extent of overlap is shown in column 4. However, a substantial amount of pHLIP coincides with Pdpn negative areas (Pdpn- area, column 5). The extent of overlap is shown in Fig 5 column 6. Severe pulmonary inflammation has been attributed to be a cause of pneumocyte death under several conditions [20-23]. Therefore, pHLIP predominantly targets lung parenchyma where there is damage to epithelial pneumocytes, and where pulmonary function is compromised.

- ***pHLIP targets lung parenchyma with diminished Prdx6 expression***

Besides gaseous exchange, pneumocytes produce several critical antioxidants to protect themselves against oxidative stress, including peroxiredoxin 6 (Prdx6), a bifunctional Glutathione (GSH) peroxidase that reduces hydrogen peroxides and lipid

hydroperoxides by utilizing GSH [24]. In previous studies, we showed that there is a transient induction of Prdx6 in ATI cells in response to infiltration, but complete disappearance of Prdx6 in consolidated alveoli possibly due to depletion of ATI cells [15]. We therefore investigated Prdx6 distribution in these studies by using fluorescent antibodies to assess the distribution of Prdx6 relative to the location of pHLIP. Prdx6 has been shown to confer significant protection against oxidative stress-induced lung injuries [25, 26]. Consistent with previous report, while Prdx6 is predominantly expressed in bronchiolar epithelial cells of uninfected mice (Fig 6A a, d, g, j), its expression is induced in alveolar epithelium of moderately infiltrated lungs where only sparsely distributed pHLIP can be found at regions neighboring heavily infiltrated sites (Fig 6A b, e, h, k). However, Prdx6 expression is severely diminished in the alveoli of heavily infiltrated/inflamed lungs (Fig 6A c, i, l). Remarkably, when pHLIP is injected in infected mice, it specifically targets regions of the lung that are deficient in Prdx6 (i.e. heavily infiltrated regions) (Fig 6A c, f, i, l). Indeed, around 90% of pHLIP-induced fluorescence resides in Prdx6-negative regions, whereas only approximately 10% of the remaining pHLIP-induced fluorescence can be found in Prdx6-positive regions (Fig 6B). The method of quantification is briefly demonstrated in Fig 6C, where the total Prdx6-positive area (Total Prdx6+ area, column 2) is identified based on anti-Prdx6 staining (Fluorescence, column 1). The percentage of pHLIP that overlaps with Prdx6-positive area (Prdx6+ pHLIP, columns 3 & 4) and Prdx6-negative area (Prdx6- pHLIP, columns 5 & 6) are then computed. These data show that pHLIP is abundant precisely where Prdx6 is deficient, suggesting opportunities for therapeutic targeting using conjugates of

pHLIP with agents that principally compensate for loss of antioxidant protection in inflamed regions of the lung.

- ***A pH-insensitive pHLIP variant targets damaged lung tissue of influenza infected mice***

Previous studies have shown that by changing two aspartates to lysines within the pHLIP sequence, the pH-dependent protonation is eliminated, rendering the peptide incapable of secondary conformation change and pH-dependent insertion into the lipid bilayer [3]. This variant sequence, termed K-pHLIP, was labeled with Hylite Fluor 647 and injected into influenza-infected mice, analogously to the pHLIP peptide. K-pHLIP cannot be protonated and thus is unresponsive to acidic pH. Indeed, unlike pHLIP, K-pHLIP does not have any significant affinity for the acidic kidney cortex (Fig S2A). Interestingly, we observed that the K-pHLIP retained at least some of its ability to target inflamed regions of the lung (Fig S2B). These data suggest the possibility that pHLIP may target damaged lung tissue due to a pH-dependent conformational change and/or via another mechanism that is pH-independent. Additional mechanisms of action may add to the robustness of pHLIP as an agent for targeting damaged lung tissue during influenza.

Discussion

Influenza-induced pneumonia is a rare, but serious pulmonary manifestation of the viral infection that is recognizable by multifocal radiographic consolidation indicating signs of cell infiltration [27]. Statistics show that patients suffering from pneumonia during 2009 H1N1 pandemic were more likely to admit into intensive care unit, suffer from acute respiratory distress syndromes (ARDS), experience sepsis and to suffer morbidity [12]. Since a general consequence of infection and inflammation is acidification of tissue, the application of the pHLIP peptide may enable specific targeting of imaging and therapeutic agents to inflamed foci of the lungs during severe influenza infections. Our objective of this study is to explore the potential utility of pHLIP in applications related to infectious diseases. Here, we report the distribution of pHLIP in influenza-infected mouse, thus revealing its potential usage as a bioimaging tool or drug delivery agent for severe influenza infections.

Our data demonstrate that pHLIP specifically directed fluorophores to damaged lung parenchyma, characterized by heavy immune cell infiltration. pHLIP targeted regions are also characterized by compromised alveoli architecture and severe depletion of a key lung antioxidant, Prdx6. The ability of pHLIP to specifically target inflamed and damaged lung tissue creates an opportunity for the delivery of pharmaceutical compounds aimed at ameliorating lung injury at the affected tissue.

A careful examination of multiple tissues showed that, consistent with previous studies, pHLIP also targets the kidneys (data not shown). Relatively little pHLIP was observed in other tissues as has been previously described. Development of pHLIP-conjugates will therefore need to take into consideration possible side effects in the

kidneys, although sodium bicarbonate can be added to the diet to increase the pH of the organs, thus reducing non-specific delivery [3].

A key finding of this study is that pHLIP specifically targets heavily infiltrated regions of influenza-infected mouse lungs. In addition, while pHLIP is appreciably detectable in the lungs during later stage of infection, it does not target infected lungs as effectively during earlier time points. This suggests that cellular or molecular events that take place during the later stage of PR8 infection create a microenvironment conducive for pHLIP targeting.

Local acidosis has been found to arise from the production of lactic acid by metabolically active polymorphonuclear cells (PMNs) [28], pHLIP targeting at the later stage of infection may be a result of lactic acid accumulation due to highly active, densely packed immune cells. Additionally, during the later stage of infection predominated by activation of the adaptive host responses, activated and proliferating T lymphocytes undergo aerobic glycolysis to meet the demand of their rapid energy consumption, thus creating a microenvironment with increased lactate [29]. This evidence is consistent with the specific targeting of pHLIP to inflamed regions of the lungs.

It is also possible that in addition to pH dependent insertion, there are additional mechanisms for pHLIP localization in infected mouse lungs. The observation that the K-pHLIP variant can target sites of inflammation during influenza suggests that these peptides share an attribute that allows for targeting in a pH-independent fashion. Studies of mice implanted with tumors show that unlike pHLIP, K-pHLIP does not target

acidic tumors, and has appreciably less distribution in the kidneys, liver, blood and spleen. However, similar distribution was observed in the lung possibly because the lung is a highly vascularized organ that has better retention of K-pHLIP [30]. Additionally, K-pHLIP is thought to have a partial α-helical structure, even at normal pH [3], and it may also form aggregates with the ability to penetrate leaky vasculature associated with inflammation. K-pHLIP might therefore become trapped in the complex milieu of the inflamed lung matrix, in a phenomenon known as the enhanced permeability and retention (EPR) effect. Regardless of the underlying mechanisms that underlie its activities, it is clear that pHLIP is highly effective in targeted sites of influenza-induced inflammation.

Potential clinical application

The selection of therapeutic agents based on the biodistribution profile of pHLIP is critical in the success of pHLIP-based drug delivery system. Localization of pHLIP specifically at regions where healthy pneumocytes are already depleted suggests that it may be too late for treatments that prevent inflammation-induced injury to lung epithelial cells. However, at this stage, the recovery of lung epithelial cells is highly critical in the survival of influenza patients. In fact, there is a growing interest in stem cell therapies or growth factors that can be exploited to facilitate regeneration of damaged lungs [16, 31, 32]. Ultimately, both traditional and novel therapeutics might be more effective when delivered with pHLIP-potentiated targeting.

The observation of pHLIP targeting Prdx6 depleted regions raises a possibility of using pHLIP to delivery agents that specifically compensate for redox imbalance caused

by Prdx6 depletion. Prdx6 has been reported to be the most critical enzyme for reducing oxidized phospholipids in the lungs [33]. Not only are oxidized phospholipids highly reactive and capable of propagating reactive oxygen species, they have also shown to mediate acute lung injury (ALI) [34] and may be involved in inducing T-cells to break tolerance towards self-protein [35]. Hence, a possible future direction is to develop pHLIP-Prdx6 conjugates to protect and restore lung tissue during influenza.

When considering factors that might impact the efficacy of pHLIP-Prdx6 conjugates, the impact of pH on Prdx6 needs to be taken into consideration. The GSH peroxidase (antioxidant) activity of Prdx6 functions maximally at physiological pH and is reduced at low pH. On the other hand, its phospholipase A_2 activity is maximal at pH 4 microenvironments, which can be found in highly acidic intracellular compartments such as lysosomes and endosomes [42]. Given that extremely low pH is unlikely to be present in the interstitium of lung tissue, one potential strategy to deliver antioxidant activity of Prdx6 but exclude phospholipase A_2 activity is to mutate a catalytic triad which is necessary for phospholipase A_2 activities [43]. Furthermore, in addition to Prdx6, there are numerous additional candidate antioxidants that can be delivered to sites of Prdx6 deficiency in order to reduce oxidative stress in influenza patients. pHLIP provides a potential vehicle for achieving this aim.

Drawing from observations of H1N1 pandemic and H5N1 avian flu patients, a significant portion of critically ill patients with viral pneumonia never recovered despite intensive care. Autopsies show that diffuse alveolar damage, intra-alveolar edema and cellular infiltration are some of the major histopathological findings [2, 36-40], which are consistent with the findings in this study. Excessive infiltration of immune cells and injury

to the lung parenchyma can compromise gaseous exchange by reducing lung volume and compliance [41]. The observation that pHLIP preferentially targets infiltrated sites suggests that conjugates that combine pHLIP with anti-inflammatory agents could be exploited to suppress oxidative stress at sites of infiltration. Importantly, targeted delivery would also reduce exposure of normal healthy portions of the lung to therapeutic agents. Given that antiinflammatory agents can be deleterious in healthy portions of the lung where they supress antiviral responsesand cause side effects, targeting is thus advantageous both because it can increase the local concentration of therapeutic agents at sites where they are needed, while at the same time preventing disruption of normal pulmonary physiology in healthy portions of the lung.

Conclusion

This study delineates the distribution of a pH-sensitive peptide, pHLIP, in a severe influenza infection model, and sets the foundation for selecting candidate agents that can be conjugated to pHLIP for therapeutic purposes. Future pandemics are inevitable. While development of new vaccines and antivirals is key, it is also important to develop alternative approaches, such as targeted drug delivery, which shows promise as a means to offset morbidity and mortality rates.

Executive summary

- Fluorescently-labelled pHLIP targets influenza-infected mouse lungs at sites of dense cellular infiltration present during the later stages of infection (85% of pHLIP colocalizes to sites of dense infiltration).
- pHLIP is detectable in close proximity to glycoproteins found on cell membranes, which suggests that pHLIP is associated with the plasma membrane.
- Approxmately 84% of fluorescently-labelled pHLIP coloclizes with tissues devoid of Pdpn-expressing ATI cells, whereas only ~16% of pHLIP is located in healthy lung tissues with Pdpn-expressing ATI cells.
- Lung tissue targeted by pHLIP has diminished Prdx6 levels, which is consistent with the depletion of ATI cells that normally express Prdx6.
- A pHLIP variant, known as K-pHLIP, which is mutated by two amino acids to render it insensitive to low pH, also localizes to inflamed lung tissue, suggesting the possibility that more than one mechanism underlies the efficacy of pHLIP targeting.

- The ability of pHLIP to effectively target inflamed regions of the lung that are deficient in antioxidants opens new therapeutic angles, including targeted delivery of antioxidants and agents that promote tissue regeneration.

Acknowledgements: We thank M.C. Phoon for propagating the virus and Dr Seet Ju Ee for her expert opinions on lung histology. This publication is made possible by the Singapore National Research Foundation and is administered by Singapore-MIT Alliance for Research and Technology. This work was also supported in part by the National Institute of Environmental Health Sciences (P01-ES006052). The views expressed herein are solely the responsibility of the authors and do not necessarily represent the official views of the Foundation. DME is supported by NIH grant GM073857.

References:

Papers of special note have been highlighted as:

* of interest

** of considerable interest

1. La Gruta NL, Kedzierska K, Stambas J, Doherty PC: A question of self-preservation: immunopathology in influenza virus infection. *Immunol Cell Biol* 85(2), 85-92 (2007).
2. Howard WA, Peiris M, Hayden FG: Report of the 'mechanisms of lung injury and immunomodulator interventions in influenza' workshop, 21 March 2010, Ventura, California, USA. *Influenza Other Respi Viruses* 5(6), 453-454, e458-475 (2011).
3.** Andreev OA, Dupuy AD, Segala M *et al.*: Mechanism and uses of a membrane peptide that targets tumors and other acidic tissues in vivo. *Proceedings of the National Academy of Sciences of the United States of America* 104(19), 7893-7898 (2007).

   ** pHLIP targets acidic tissues such as tumours and arthritic joints.

4. Segala J, Engelman DM, Reshetnyak YK, Andreev OA: Accurate analysis of tumor margins using a fluorescent pH Low Insertion Peptide (pHLIP). *International journal of molecular sciences* 10(8), 3478-3487 (2009).
5. Andreev OA, Engelman DM, Reshetnyak YK: Targeting acidic diseased tissue: New technology based on use of the pH (Low) Insertion Peptide (pHLIP). *Chimica oggi* 27(2), 34-37 (2009).
6. Reshetnyak YK, Yao L, Zheng S, Kuznetsov S, Engelman DM, Andreev OA: Measuring Tumor Aggressiveness and Targeting Metastatic Lesions with Fluorescent pHLIP. *Mol Imaging Biol*, (2010).
7.* Reshetnyak YK, Andreev OA, Lehnert U, Engelman DM: Translocation of molecules into cells by pH-dependent insertion of a transmembrane helix. *Proceedings of the National Academy of Sciences of the United States of America* 103(17), 6460-6465 (2006).

   The biophysical properties of pHLIP enables it to either thether molecules on the extracellular surface of plasma membrane or translocate molecules across the cell membrane into the cytosol.

8. An M, Wijesinghe D, Andreev OA, Reshetnyak YK, Engelman DM: pH-(low)-insertion-peptide (pHLIP) translocation of membrane impermeable phalloidin toxin inhibits cancer cell proliferation. *Proceedings of the National Academy of Sciences of the United States of America* 107(47), 20246-20250 (2010).
9. Thevenin D, An M, Engelman DM: pHLIP-mediated translocation of membrane-impermeable molecules into cells. *Chemistry & biology* 16(7), 754-762 (2009).
10. Punnia-Moorthy A: Evaluation of pH changes in inflammation of the subcutaneous air pouch lining in the rat, induced by carrageenan, dextran and Staphylococcus aureus. *J Oral Pathol* 16(1), 36-44 (1987).
11. Martin GR, Jain RK: Fluorescence ratio imaging measurement of pH gradients: calibration and application in normal and tumor tissues. *Microvasc Res* 46(2), 216-230 (1993).

12. Jain S, Benoit SR, Skarbinski J, Bramley AM, Finelli L: Influenza-Associated Pneumonia Among Hospitalized Patients With 2009 Pandemic Influenza A (H1N1) Virus--United States, 2009. *Clin Infect Dis* 54(9), 1221-1229 (2012).
13. Buchweitz JP, Harkema JR, Kaminski NE: Time-dependent airway epithelial and inflammatory cell responses induced by influenza virus A/PR/8/34 in C57BL/6 mice. *Toxicol Pathol* 35(3), 424-435 (2007).
14. Srivastava B, Blazejewska P, Hessmann M *et al.*: Host genetic background strongly influences the response to influenza a virus infections. *PLoS One* 4(3), e4857 (2009).
15. Yamada Y, Limmon GV, Zheng D *et al.*: Major Shifts in the Spatio-Temporal Distribution of Lung Antioxidant Enzymes during Influenza Pneumonia. *PLoS One* 7(2), e31494 (2012).
16. Kumar PA, Hu Y, Yamamoto Y *et al.*: Distal airway stem cells yield alveoli in vitro and during lung regeneration following H1N1 influenza infection. *Cell* 147(3), 525-538 (2011).
17. Andreev OA, Karabadzhak AG, Weerakkody D, Andreev GO, Engelman DM, Reshetnyak YK: pH (low) insertion peptide (pHLIP) inserts across a lipid bilayer as a helix and exits by a different path. *Proceedings of the National Academy of Sciences of the United States of America* 107(9), 4081-4086 (2010).
18. Reshetnyak YK, Andreev OA, Segala M, Markin VS, Engelman DM: Energetics of peptide (pHLIP) binding to and folding across a lipid bilayer membrane. *Proc Natl Acad Sci U S A* 105(40), 15340-15345 (2008).
19. Narasaraju T, Ng HH, Phoon MC, Chow VT: MCP-1 antibody treatment enhances damage and impedes repair of the alveolar epithelium in influenza pneumonitis. *Am J Respir Cell Mol Biol* 42(6), 732-743 (2010).
20. Perl M, Lomas-Neira J, Chung CS, Ayala A: Epithelial cell apoptosis and neutrophil recruitment in acute lung injury-a unifying hypothesis? What we have learned from small interfering RNAs. *Mol Med* 14(7-8), 465-475 (2008).
21. Smani Y, Docobo-Perez F, Mcconnell MJ, Pachon J: Acinetobacter baumannii-induced lung cell death: role of inflammation, oxidative stress and cytosolic calcium. *Microb Pathog* 50(5), 224-232 (2011).
22. Rock KL: Pathobiology of inflammation to cell death. *Biol Blood Marrow Transplant* 15(1 Suppl), 137-138 (2009).
23. Bergeron Y, Ouellet N, Deslauriers AM, Simard M, Olivier M, Bergeron MG: Cytokine kinetics and other host factors in response to pneumococcal pulmonary infection in mice. *Infect Immun* 66(3), 912-922 (1998).
24. Fisher AB: Peroxiredoxin 6: a bifunctional enzyme with glutathione peroxidase and phospholipase A activities. *Antioxid Redox Signal* 15(3), 831-844 (2011).
25. Wang Y, Phelan SA, Manevich Y, Feinstein SI, Fisher AB: Transgenic mice overexpressing peroxiredoxin 6 show increased resistance to lung injury in hyperoxia. *Am J Respir Cell Mol Biol* 34(4), 481-486 (2006).
26. Yang D, Song Y, Wang X *et al.*: Deletion of peroxiredoxin 6 potentiates lipopolysaccharide-induced acute lung injury in mice. *Crit Care Med* 39(4), 756-764 (2011).
27. Nicolini A, Ferrera L, Rao F, Senarega R, Ferrari-Bravo M: Chest radiological findings of influenza A H1N1 pneumonia. *Rev Port Pneumol*, (2012).
28. Menkin V: Biochemical Mechanisms in Inflammation. *Br Med J* 1(5185), 1521-1528 (1960).
29. Frauwirth KA, Thompson CB: Regulation of T lymphocyte metabolism. *J Immunol* 172(8), 4661-4665 (2004).
30. Daumar P, Wanger-Baumann CA, Pillarsetty N *et al.*: Efficient (18)F-Labeling of Large 37-Amino-Acid pHLIP Peptide Analogues and Their Biological Evaluation. *Bioconjugate chemistry* 23(8), 1557-1566 (2012).

31. Yanagita K, Matsumoto K, Sekiguchi K, Ishibashi H, Niho Y, Nakamura T: Hepatocyte growth factor may act as a pulmotrophic factor on lung regeneration after acute lung injury. *The Journal of biological chemistry* 268(28), 21212-21217 (1993).
32. Rennard SI, Wachenfeldt K: Rationale and emerging approaches for targeting lung repair and regeneration in the treatment of chronic obstructive pulmonary disease. *Proceedings of the American Thoracic Society* 8(4), 368-375 (2011).
33. Liu G, Feinstein SI, Wang Y *et al.*: Comparison of glutathione peroxidase 1 and peroxiredoxin 6 in protection against oxidative stress in the mouse lung. *Free Radic Biol Med* 49(7), 1172-1181 (2010).
34. Imai Y, Kuba K, Neely GG *et al.*: Identification of oxidative stress and Toll-like receptor 4 signaling as a key pathway of acute lung injury. *Cell* 133(2), 235-249 (2008).
35. Wuttge DM, Bruzelius M, Stemme S: T-cell recognition of lipid peroxidation products breaks tolerance to self proteins. *Immunology* 98(2), 273-279 (1999).
36. Valente T, Lassandro F, Marino M, Squillante F, Aliperta M, Muto R: H1N1 pneumonia: our experience in 50 patients with a severe clinical course of novel swine-origin influenza A (H1N1) virus (S-OIV). *Radiol Med* 117(2), 165-184 (2012).
37. Soepandi PZ, Burhan E, Mangunnegoro H *et al.*: Clinical course of avian influenza A(H5N1) in patients at the Persahabatan Hospital, Jakarta, Indonesia, 2005-2008. *Chest* 138(3), 665-673 (2010).
38. Bay A, Etlik O, Oner AF *et al.*: Radiological and clinical course of pneumonia in patients with avian influenza H5N1. *Eur J Radiol* 61(2), 245-250 (2007).
39. Nakajima N, Sato Y, Katano H *et al.*: Histopathological and immunohistochemical findings of 20 autopsy cases with 2009 H1N1 virus infection. *Mod Pathol* 25(1), 1-13 (2012).
40. Korteweg C, Gu J: Pathology, molecular biology, and pathogenesis of avian influenza A (H5N1) infection in humans. *Am J Pathol* 172(5), 1155-1170 (2008).
41. Korotzer TI, Weiss HS, Hamparian VV, Somerson NL: Oxygen uptake and lung function in mice infected with Streptococcus pneumoniae, influenza virus, or Mycoplasma pulmonis. *J Lab Clin Med* 91(2), 280-294 (1978).
42. Wu YZ, Manevich Y, Baldwin JL *et al.*: Interaction of surfactant protein A with peroxiredoxin 6 regulates phospholipase A2 activity. *The Journal of biological chemistry* 281(11), 7515-7525 (2006).
43. Manevich Y, Shuvaeva T, Dodia C, Kazi A, Feinstein SI, Fisher AB: Binding of peroxiredoxin 6 to substrate determines differential phospholipid hydroperoxide peroxidase and phospholipase A(2) activities. *Archives of biochemistry and biophysics* 485(2), 139-149 (2009).

Figure Legends

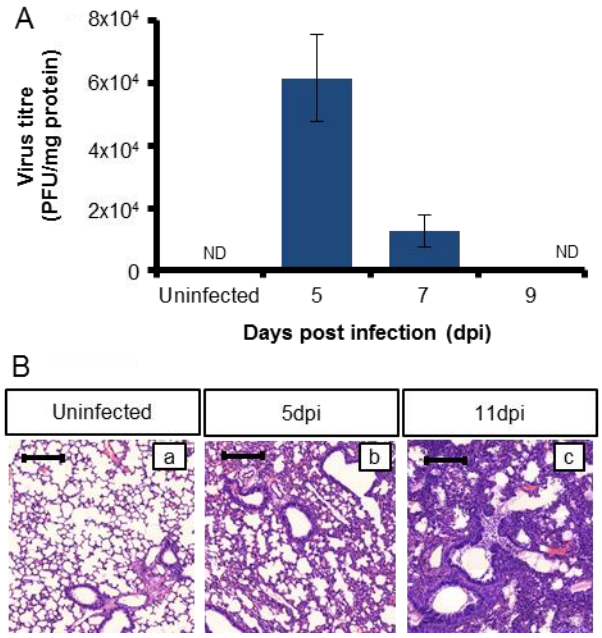

Fig 1. A) Quantification of viral plaques from lung homogenate. Plaque forming units (PFU) are normalized to mg protein in the lung homogenates (measured by Bradford assay) and represented as PFU ± SD. B) Prolonged inflammation in the lungs of PR8 infected mice. Representative H&E diagrams show (a) normal alveolar structure in uninfected mouse lung, (b) thickening of alveolar walls with infiltration of immune cells on 5 dpi and (c) severe lung infiltration and disrupted alveolar structures on 11 dpi, after virus has been cleared *(n* = 3). Scale bar = 200µm. dpi = days post infection.

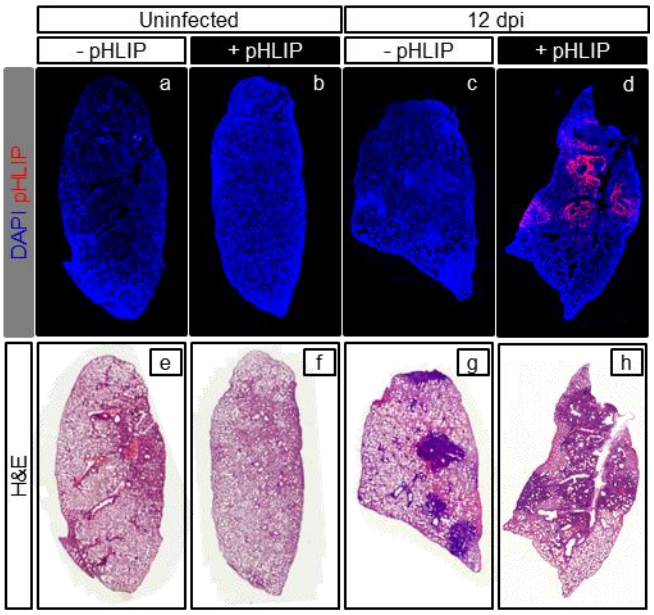

Fig 2. pHLIP targets infected but not uninfected mouse lungs. Representative whole lung images from three independent experiments ($n \geq 4$). pHLIP was administered to PR8-infected mice on day 10 post infection. Top: DAPI (blue) and pHLIP (red). (b, d) On 12 dpi, pHLIP can only be detected in infected lungs. (a, c) Control lungs from uninfected and infected mice. Bottom: H&E staining of the same samples. Darkened areas indicate regions of immune cell infiltration and inflammation.

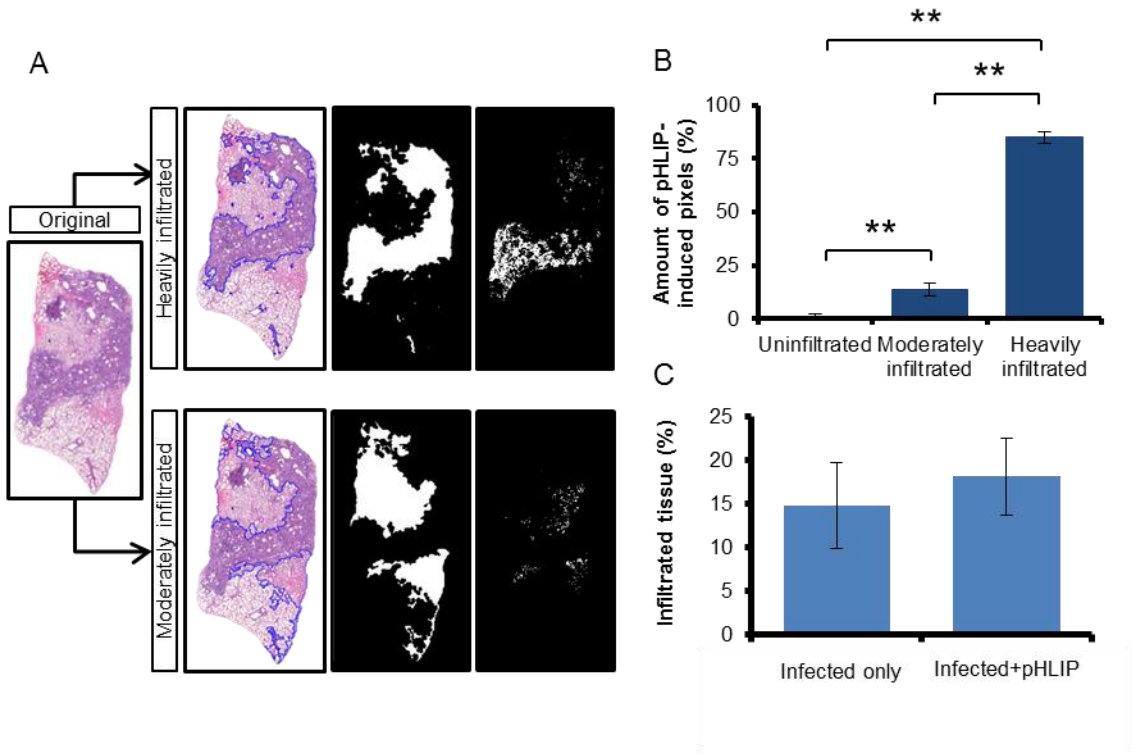

Fig 3. A) Method of quantification for pHLIP in different regions of the lungs. Original H&E images (left column) were segmented to distinguish heavily infiltrated and moderately infiltrated regions, which are traced in blue lines in the second column. Alveoli, bronchi and blood vessels were filled to generate an alveolar area as shown in the third column. The total amount of pHLIP-induced fluorescence that overlaps with these alveolar areas (as shown in right column) was then quantified. ~~Original H&E images (left most) were segmented to distinguish heavily infiltrated and moderately infiltrated regions which are traced out in blue lines (right panels; left most images on the top and bottom respectively). Alveolar, bronchiolar or blood vessels were filled to generate masks over these regions (right panels; center images). Total amount of pHLIP-induced fluorescence found in these regions were then quantified in overlapping fluorescence images of the same tissue sections (right panels; right images).~~ B) pHLIP

most preferentially targets heavily infiltrated regions. Only 1.4 ± 0.7 % of total pHLIP was found in uninfiltrated regions, while 13.7 ± 2.9% of pHLIP was found in moderately infiltrated regions and 84.9 ± 2.7% of pHLIP was found in heavily infiltrated regions. Percentage of pHLIP in different regions were calculated using two lung sections per mouse (n = 3). Bars indicate SEM. **p< 0.01 (Student's t-test). C) pHLIP injection does not affect the degree of infiltration into mice lungs. Ten 5 µm thick lung sections at least 50 µm apart were obtained from infected mice injected or not injected with Hylite-Fluor 647 pHLIP. They were stained with H&E and the percentage of heavily infiltrated tissue are quantified (n=5). Data show that there is no significant difference between percentages of infiltration between these two groups.

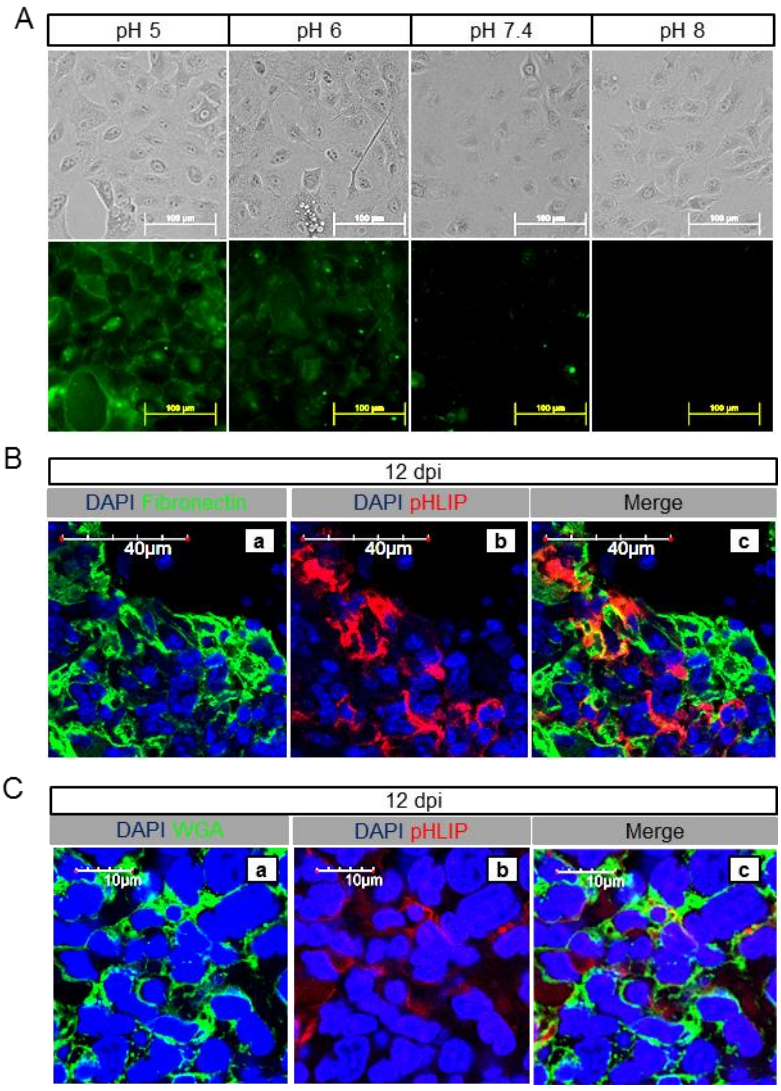

Fig 4 A) pHLIP preferentially binds cell membrane at acidic pH *in vitro*. A549 cells were incubated with 8μM of 5-FAM conjugated pHLIP under different pH conditions. 5-FAM conjugated pHLIP binds cell membrane of A549 cells at acidic pH of pH 5 and pH 6, but not at alkaline pH of pH 7.4 and pH8. B) Fibrillar fibronectin (green) delineates extracellular space where some pHLIP (red) can be found (60x magnification). C) pHLIP is in close proximity to WGA-stained cell membrane glycoprotein (100x magnification). WGA stains the cell membrane (green) of influenza-infected mice lungs. In the heavily infiltrated regions, thin streaks of pHLIP (red) run around the perimeter of cells and are

sandwiched by or colocalize with WGA-staining suggesting close proximity to the cell membrane.

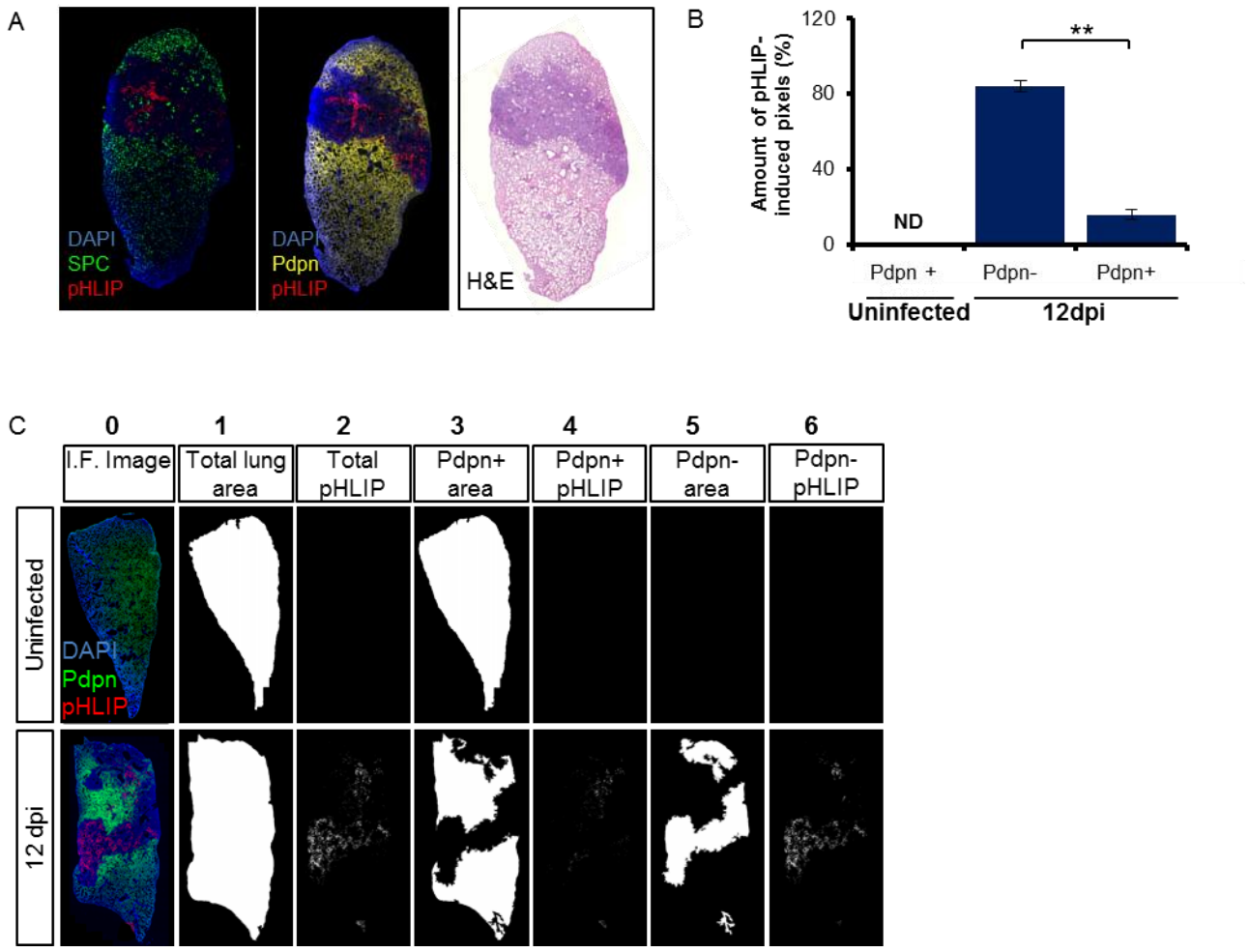

Fig 5. A) pHLIP targets damaged lung tissue devoid of normal ATII and ATI cells. Representative images of lungs sections stained with anti-SPC and anti-Pdpn. pHLIP (red) does not colocalize with SPC-positive ATII (green) or Pdpn-positive ATI cells (yellow). B) pHLIP is mostly observed in regions devoid of Pdpn-positive ATI. The percentages of pHLIP-positive pixels in Pdpn-positive (Pdpn+) and Pdpn-negative (Pdpn-) regions were calculated using two lung sections per mouse (*n* = 3). There are significantly more pHLIP-induced pixels in Pdpn-negative regions (84.1 ± 2.7%) as compared to Pdpn-positive regions (15.9 ± 2.7%) of PR8-infected mice. Bars indicate

SEM. **p< 0.01 (Student's t-test). C) Coincidence of pHLIP positive regions and Pdpn+ and Pdpn- regions. Total area of lung sections (column 1) according to DAPI staining (column 0). Pdpn+ area (column 3) and Pdpn-negative areas (column 5) were imaged and quantified according to Pdpn immunohistochemistry. Total pHLIP staining is shown in column 2 and pHLIP staining that coincides with Pdpn+ or Pdpn- regions are shown in columns 4 and 6 respectively.

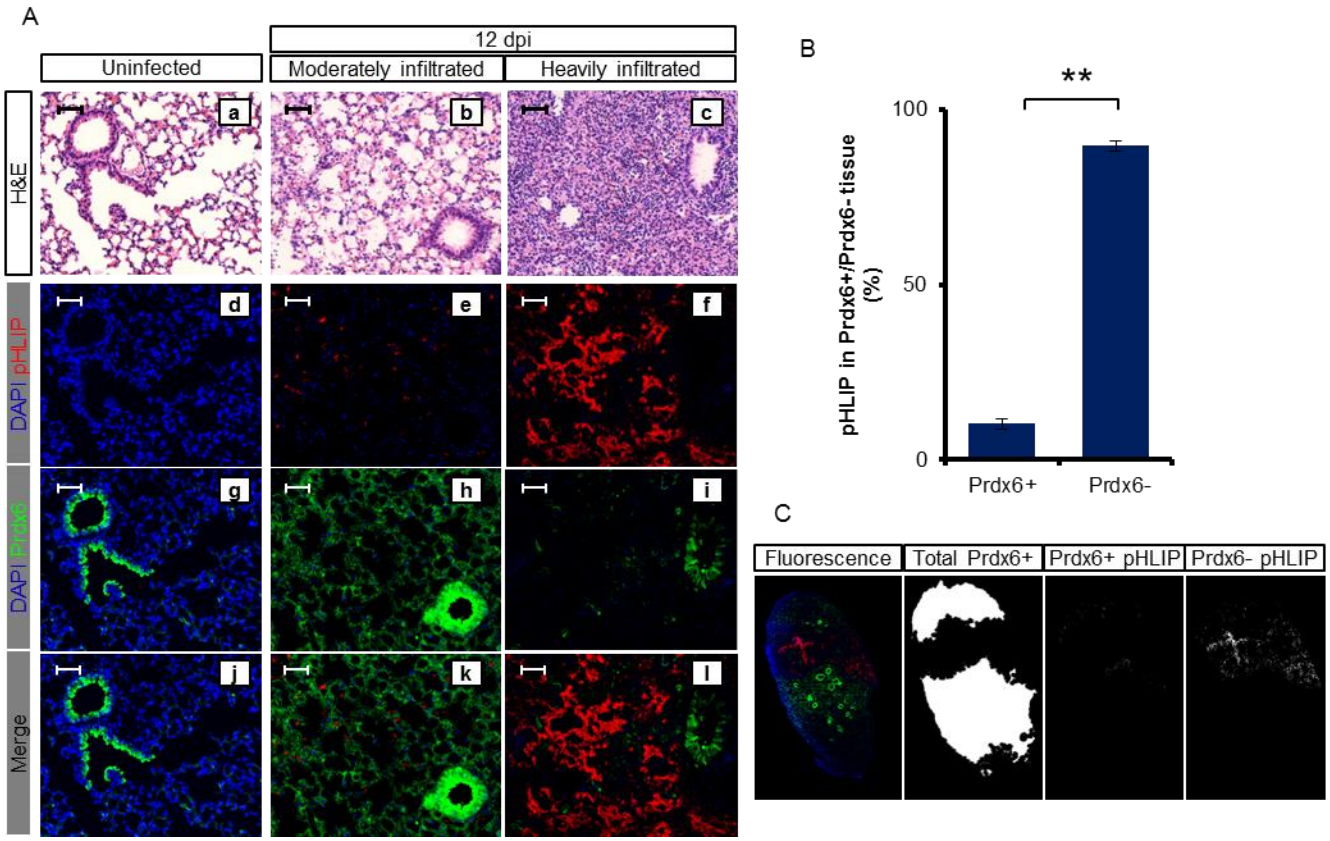

Fig 6. A) pHLIP localizes at lung tissue depleted of Prdx6. (a, g, j) Prdx6 (green) is expressed at baseline level in the alveolar epithelium of uninfected-mouse lungs. (d) No pHLIP was found in the uninfected lung tissue. (b, h, k) Prdx6 is elevated in moderately infiltrated tissue of infected mouse lungs, ~~(e, k)~~ where (e, k) ~~-~~sparsely distributed pHLIP can only be found at sites immediately neighbouring heavily infiltrated tissue. (c, f, i, l)

pHLIP mainly targets inflamed sites with diminished Prdx6 expression both in the alveolar and the bronchiolar epithelial cells. Scale bar = 100 μm. B) The percentages of pHLIP fluorescence in Prdx6-positive (Prdx6+) and Prdx6-negative (Prdx6-) regions are calculated with two immunofluorescently-labeled lung sections per mouse (*n* = 3). pHLIP-induced pixels are almost exclusively found in Prdx6- regions (89.7 ± 3.3%). Significantly less pHLIP can be detected in Prdx6+ regions (10.3 ± 3.3%) of PR8-infected mice. Bars are shown as mean± SEM. ** $p<0.01$ for percent of pHLIP-induced fluorescence in Prdx6+ lung tissue as compared to Prdx6- lung tissue in PR8-infected mice. C) Coincidence of pHLIP fluorescence with regions of Prdx6 immunofluorescence was identified. Fluorescence image of whole lung section stained with anti-Prdx6 (column 1) was quantified by separating Prdx6 (green) and pHLIP (red) channels. Prdx6+ regions are identified (column 2) and percentages of pHLIP residing in Prdx6+ (column 3) and prdx6- (column 4) regions were quantified.

Supplementary figures

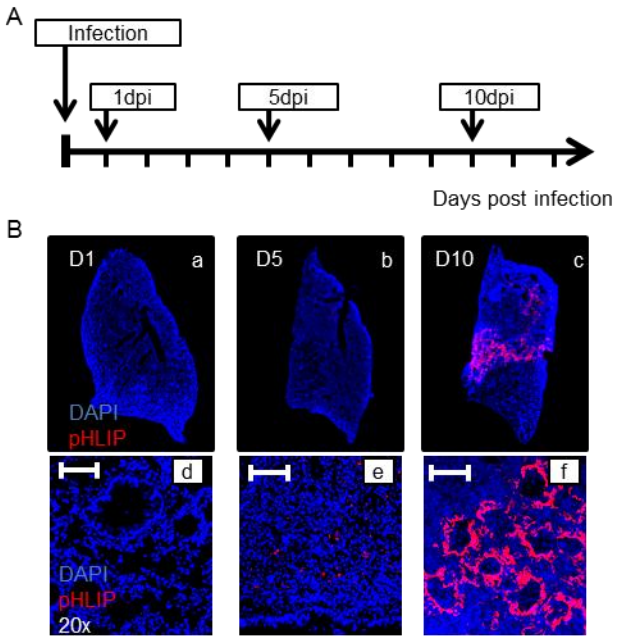

Suppl. Figure 1) pHLIP localized in inflamed site of infected-mouse lungs during later stage of infection but not during the early stage of infections. A) Timeline indicating times for pHLIP administration B) (a, b, d, e) pHLIP is not detected when administered day 1 post infection (D1) but was observed in 1 out of 3 mice when administered on day 5 post infection (D5). (c, f) pHLIP fluorescence can be consistently detected in infected lungs when injected on day 10 post infection (D10).

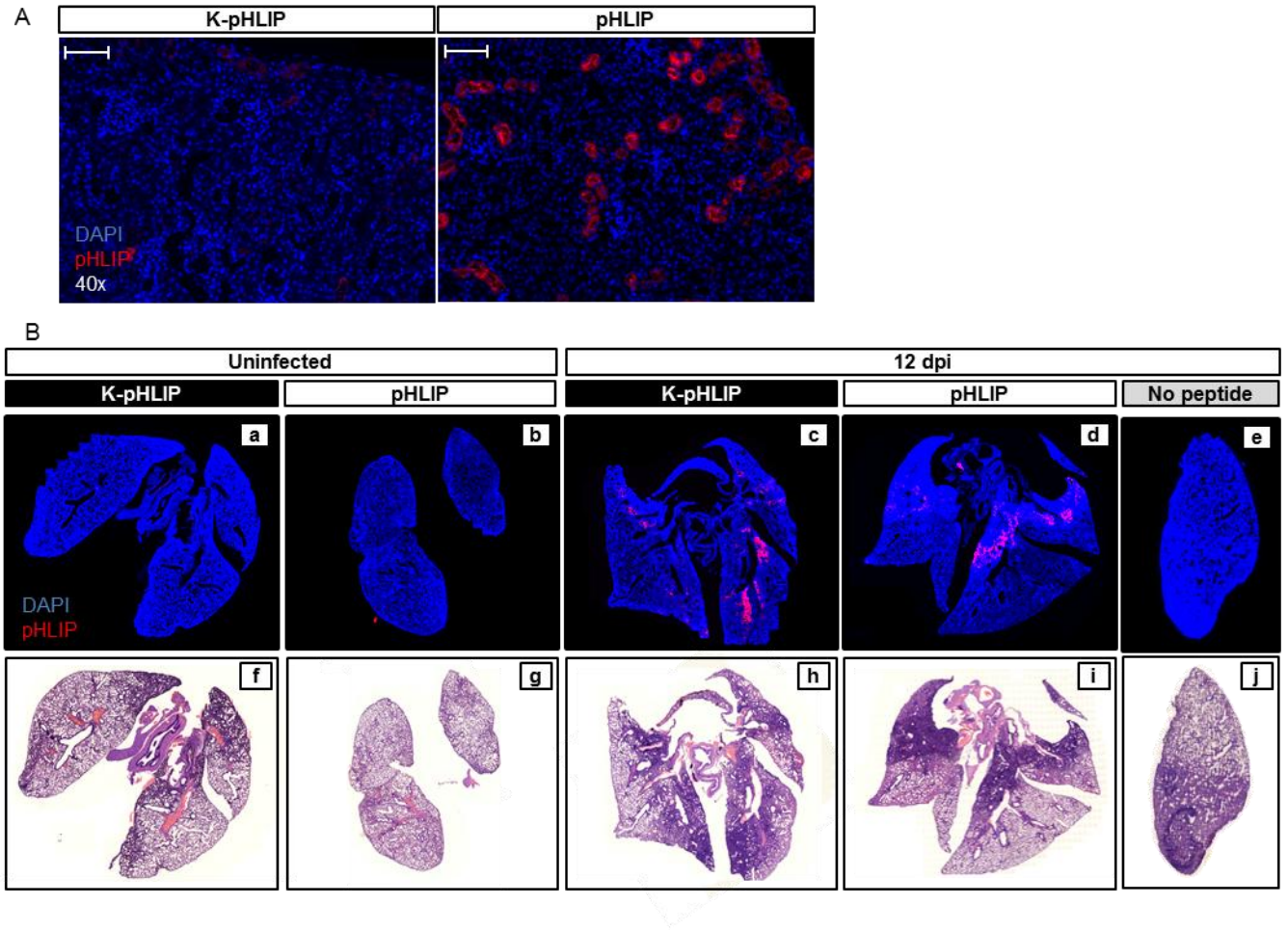

Suppl. Figure 2A) K-pHLIP has very little affinity for the acidic cortex of kidneys (left), whereas pHLIP readily targets the kidney (right). Scale bar = 50 µm. B) K-pHLIP targets damaged lung tissue. Similar to pHLIP, Hylite fluor 647-conjugated K-pHLIP does not target uninfected mouse lungs (a, b, f, g) but localizes at heavily infiltrated regions of infected mouse lungs (c, d, h, i). Mice that did not receive any peptides served as negative controls (e, j) ($n \geq 4$).

Fig 1

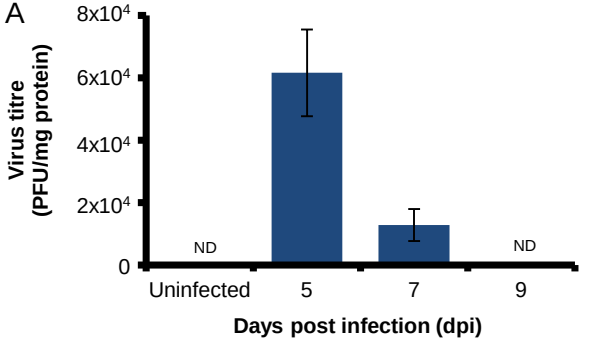
A
8x10⁴
6x10⁴
4x10⁴
2x10⁴
0
Virus titre (PFU/mg protein)
ND
ND
Uninfected
5
7
9
Days post infection (dpi)
B
Uninfected
5dpi
11dpi
a
b
c

Fig 2

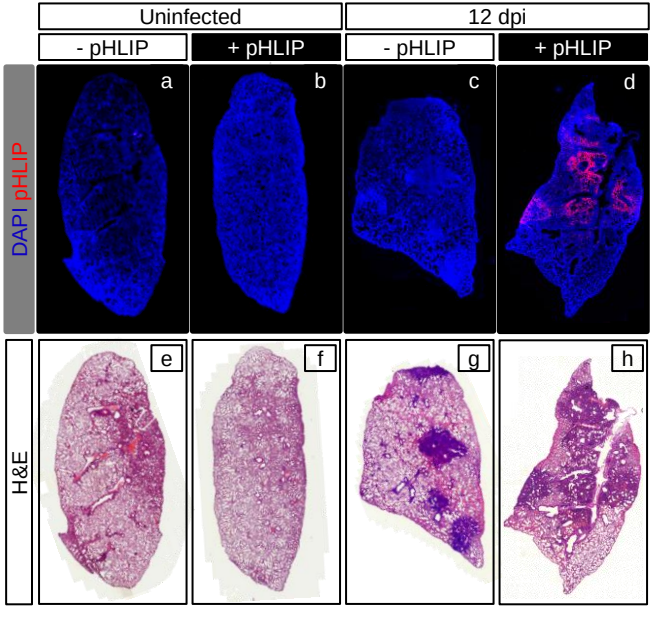
Uninfected
12 dpi
- pHLIP
+ pHLIP
- pHLIP
+ pHLIP
DAPI pHLIP
a
b
c
d
H&E
e
f
g
h

Fig 3

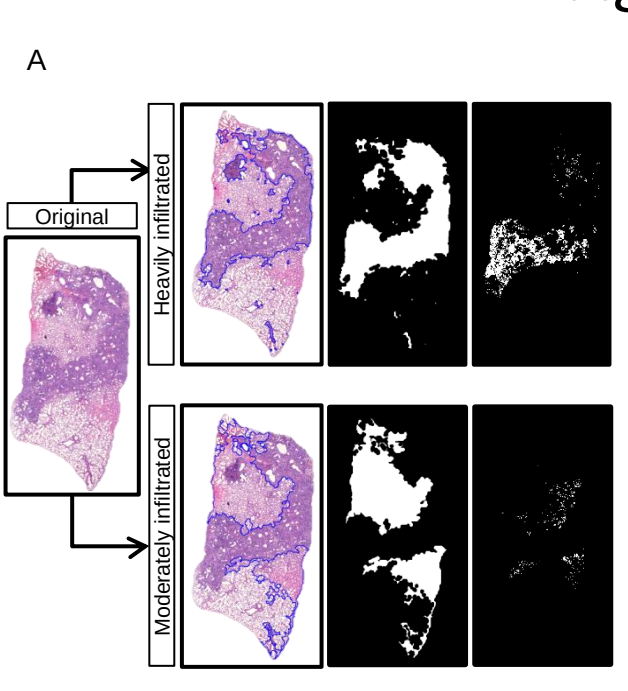
A
Original
Heavily infiltrated
Moderately infiltrated

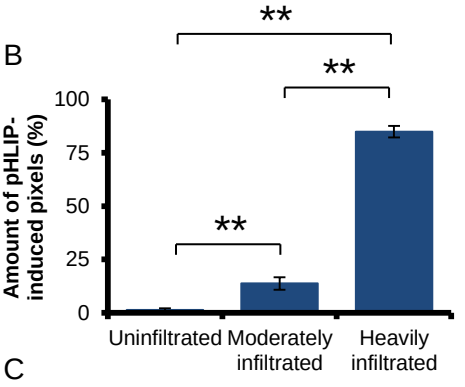
B
**
**
**
Amount of pHLIP-induced pixels (%)
100
75
50
25
0
Uninfiltrated
Moderately infiltrated
Heavily infiltrated

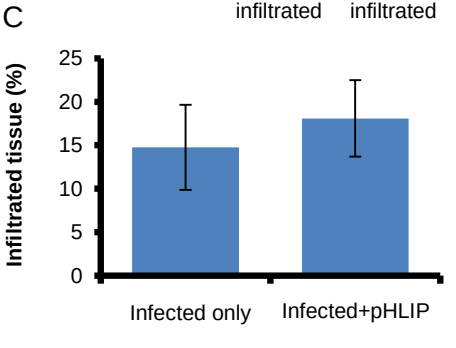
C
Infiltrated tissue (%)
25
20
15
10
5
0
Infected only
Infected+pHLIP

Fig 4

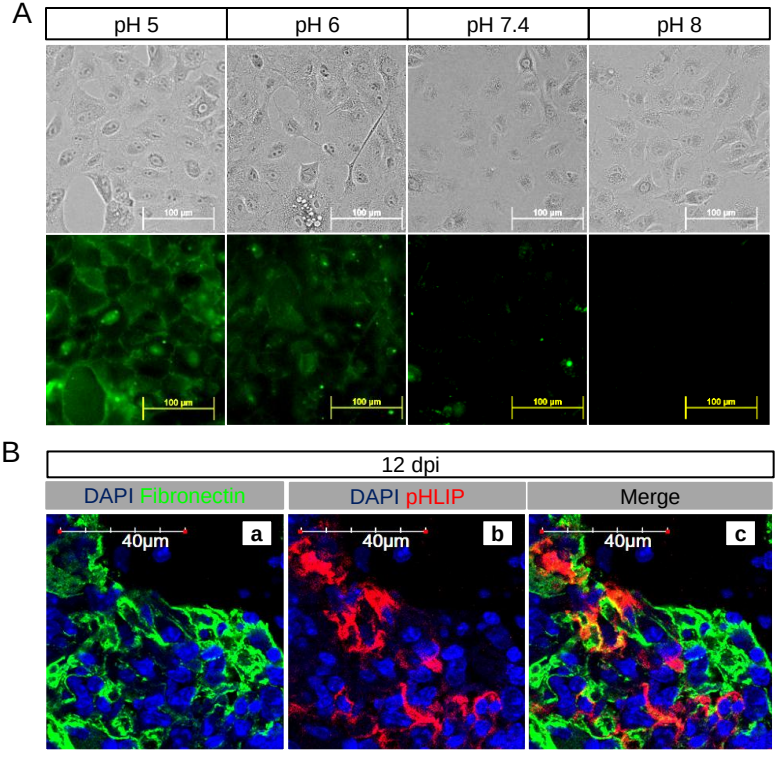
A
pH 5
pH 6
pH 7.4
pH 8
100 µm
B
12 dpi
DAPI Fibronectin
DAPI pHLIP
Merge
40µm
a
40µm
b
40µm
c

Fig 4

C

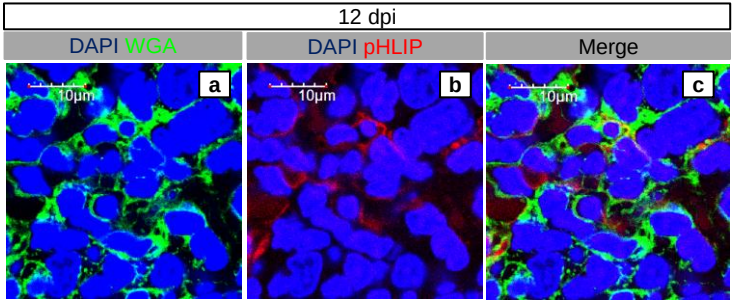

Fig 5

A

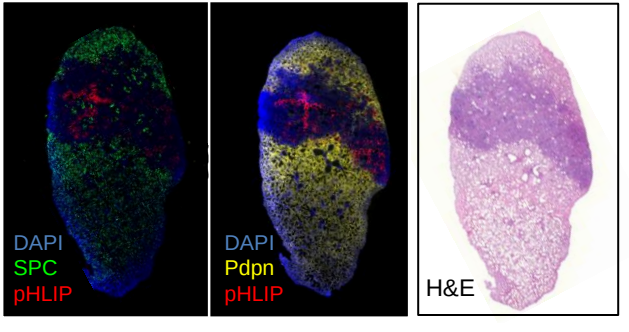
DAPI
SPC
pHLIP
DAPI
Pdpn
pHLIP
H&E

B

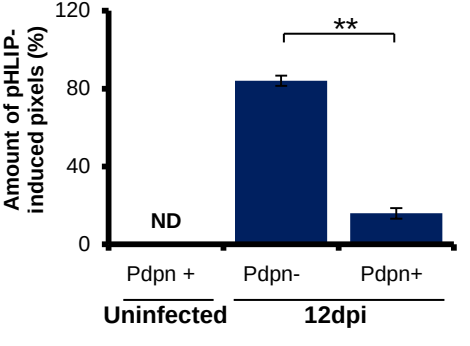
Amount of pHLIP-induced pixels (%)
120
80
40
0
**
ND
Pdpn +
Pdpn-
Pdpn+
Uninfected
12dpi

Fig 5

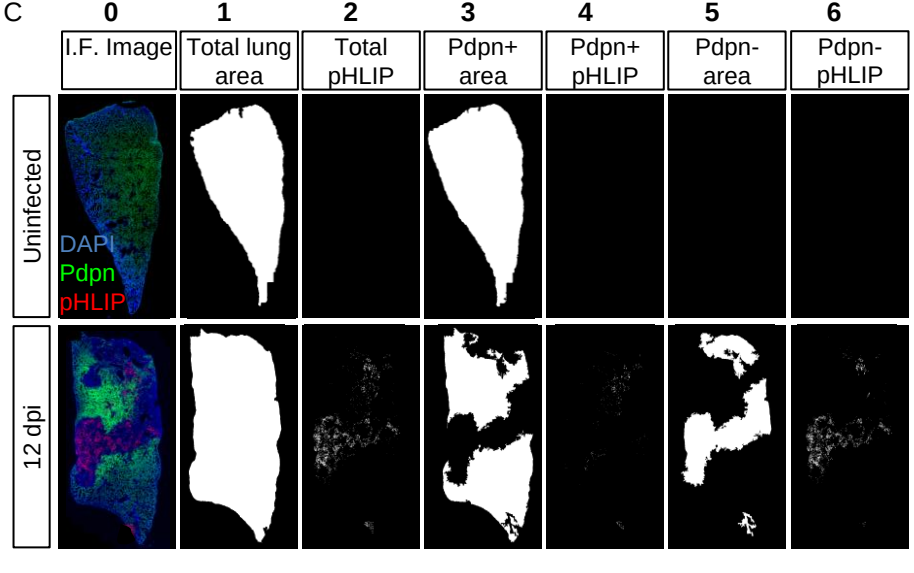
C
0
1
2
3
4
5
6
I.F. Image
Total lung area
Total pHLIP
Pdpn+ area
Pdpn+ pHLIP
Pdpn- area
Pdpn- pHLIP
Uninfected
12 dpi
DAPI
Pdpn
pHLIP

Fig 6

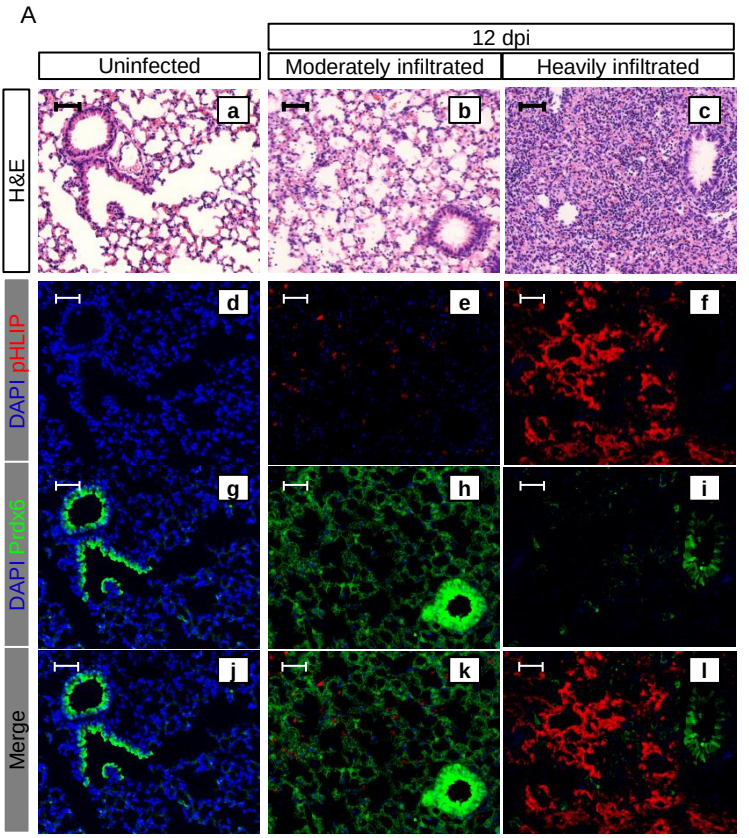
A
12 dpi
Uninfected
Moderately infiltrated
Heavily infiltrated
H&E
DAPI pHLIP
DAPI Prdx6
Merge
a
b
c
d
e
f
g
h
i
j
k
l

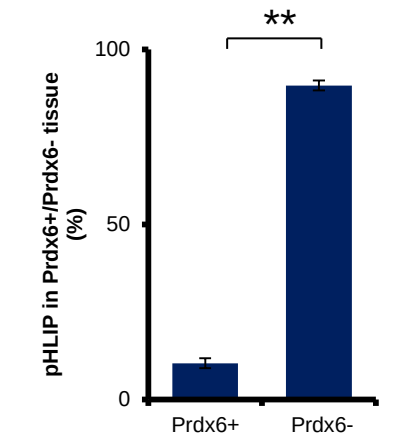
B
**
100
50
0
pHLIP in Prdx6+/Prdx6- tissue (%)
Prdx6+
Prdx6-

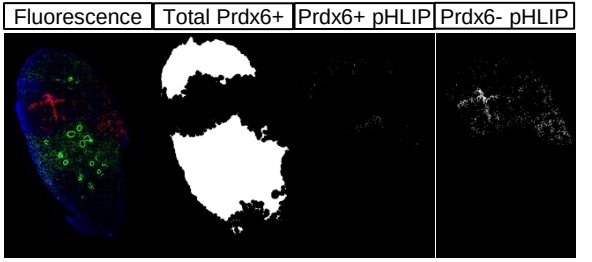
C
Fluorescence
Total Prdx6+
Prdx6+ pHLIP
Prdx6- pHLIP

Suppl. Fig 1

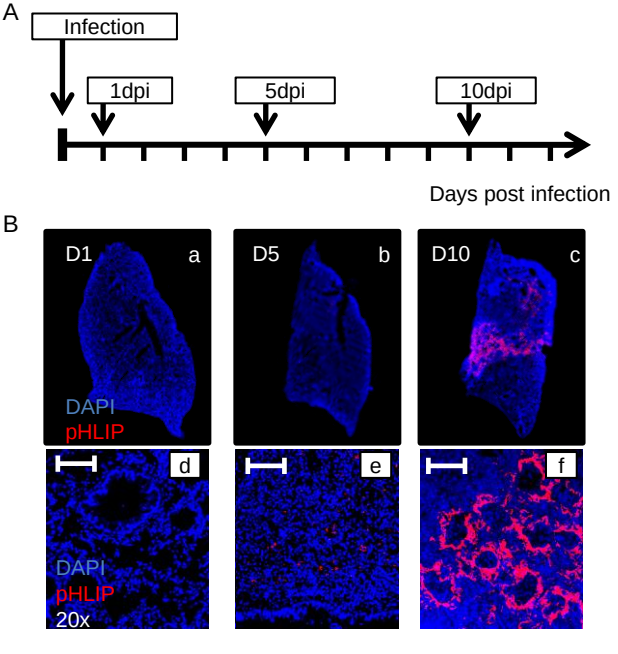
A
Infection
1dpi
5dpi
10dpi
Days post infection
B
D1
a
D5
b
D10
c
DAPI
pHLIP
d
e
f
DAPI
pHLIP
20x

Suppl. Fig 2

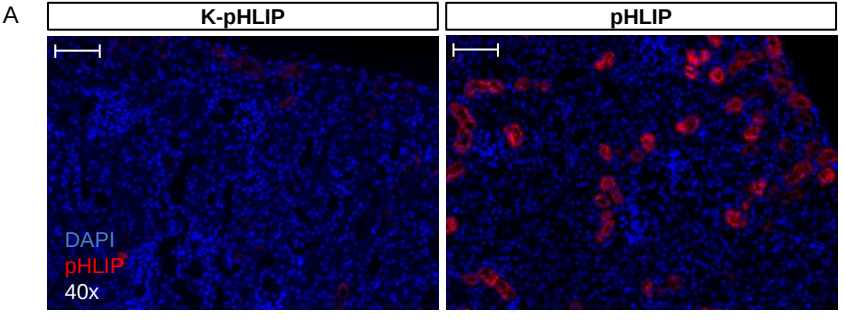

Suppl. Fig 2

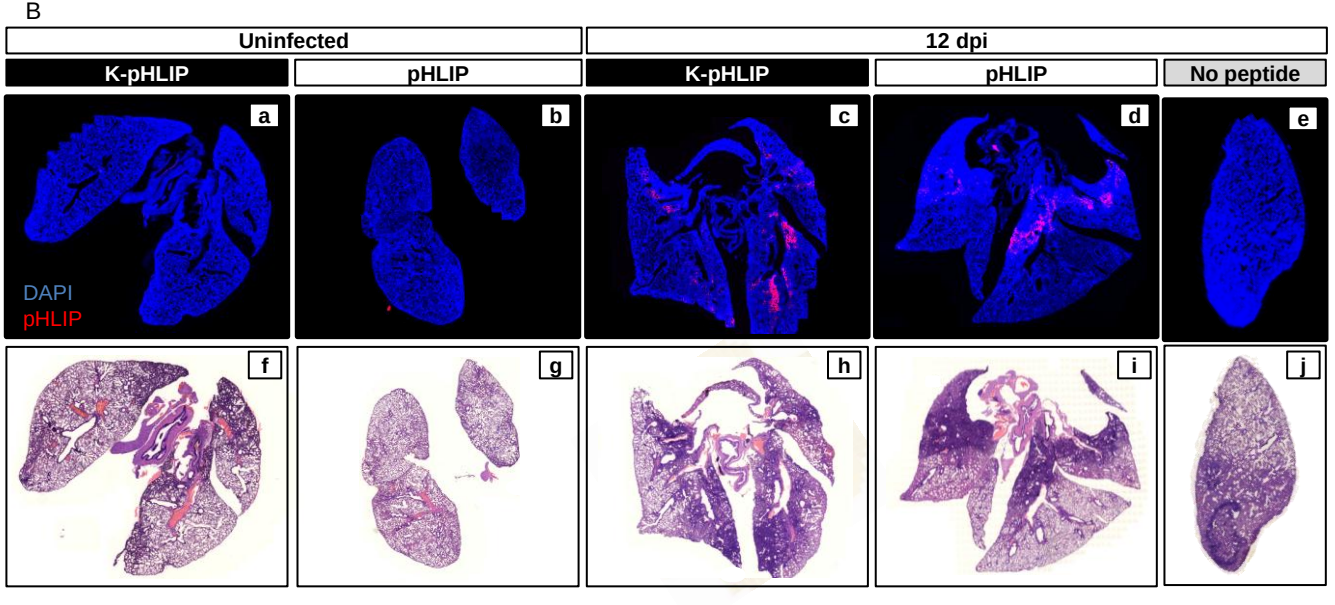
B
Uninfected
12 dpi
K-pHLIP
pHLIP
K-pHLIP
pHLIP
No peptide
a
b
c
d
e
DAPI
pHLIP
f
g
h
i
j